Probing Disordered Substrates by Imaging the Adsorbate in its Fluid Phase

Ankush Sengupta* and Surajit Sengupta†

S.N. Bose National Centre for Basic Sciences,

Block JD, Sector III, Salt Lake,

Kolkata 700 098,

India.

Gautam I. Menon‡

The Institute of Mathematical Sciences,

C.I.T. Campus, Taramani,

Chennai 600 113,

India.

(Dated: February 2, 2008)

Abstract

Several recent imaging experiments access the equilibrium density profiles of interacting particles confined to a two-dimensional substrate. When these particles are in a fluid phase, we show that such data yields precise information regarding substrate disorder as reflected in one-point functions and two-point correlations of the fluid. Using Monte Carlo simulations and replica generalizations of liquid state theories, we extract unusual two-point correlations of time-averaged density inhomogeneities induced by disorder. Distribution functions such as these have not hitherto been measured but should be experimentally accessible.

PACS numbers: 68.43.De,79.60.Ht,61.20.-p,05.20.Jj

* E-mail : ankush@bose.res.in

† E-mail : surajit@bose.res.in

‡ E-mail : menon@imsc.res.in

Place a perfect crystal in a disordered background deriving from a large number of randomly placed, quenched point pinning sites. Allow the crystal to relax to its minimum free energy state in this background. A qualitative picture of structure in the state which results is obtained by balancing the energy cost of distortions in the displacement field with the energy gained from accomodating locally to the pinning, a competition conventionally described via the paradigm of an elastic manifold in a random medium [1, 2]. Such a starting point, however, is clearly inadequate when equilibrium correlations in the pure system do not resemble those of a crystal or indeed of any system in which particles of fixed connectivity are separated by a mean distance from which deviations are energetically penalized. The appropriate problem in this case is that of determining the correlations of an *equilibrium* fluid in a quenched random environment[3]. Such a description applies to a large number of experimental systems. Indeed, systems modelled as elastic manifolds at low temperatures generically melt into fluid states at high enough temperatures.

Equilibrium fluids in a quenched disordered background exhibit disorder-averaged versions of the conventional correlation functions of the pure system. In addition, new classes of non-trivial correlations emerge [3]. Modern imaging techniques enable direct microscopic visualization of several two-dimensional situations which may be mapped onto the problem of interest here: these include colloidal particles in their fluid phase on rough substrates[4, 5, 6], magnetic bubble domain arrays at large effective temperatures[7], charge-density wave systems[8] and varied phases of vortices in thin superconducting films[9, 10, 11, 12, 13]. As we show in this Letter, such experiments raise the possibility of measuring novel correlation functions associated with fluid systems in the presence of quenched disorder. In addition, the topography of surface randomness can be accessed from the images yielded by such methods, even though it is the fluid (adsorbate) particles which are being imaged and not the substrate directly.

This Letter describes a procedure for reconstituting a disorder potential in microscopic detail from knowledge of the time averaged density $\rho(\mathbf{r})$ of the adsorbate in the liquid state and its spatial correlations. To this end, we also present accurate benchmarks for replica-based liquid state theories for correlations in disordered systems, comparing the predictions of these theories with direct simulations. Our proposals are illustrated using Monte Carlo computer experiments on a model two-dimensional fluid in a disordered background. Figure 1 exhibits our main result: Fig.1 (a) shows the random substrate potential used in our

FIG. 1: (color-online) (a) Color plot of the disorder potential $\beta V_d(x, y)$ used in our Monte Carlo simulation. The plot is a single realization of a Gaussian random potential of strength $\sigma^2 = .1$ and correlation length $\xi = .12\sigma_0$. (b) The reconstituted potential (see text) with the measured time averaged density $\rho(\mathbf{r})$ (Fig. 2 (a)) as input. The correspondence between (a) and (b) is close but can be systematically improved by averaging $\rho(\mathbf{r})$ for longer times. The σ^2 and ξ obtained from (b) agree with the input values in (a) to within a few percent.

Monte Carlo calculations, while Fig. 1 (b) exhibits the reconstituted potential obtained from the *induced* $\rho(\mathbf{r})$, using a replica-based liquid state theory [3]. As these figures illustrate, to an accuracy limited only by the computational effort required for a well-averaged $\rho(\mathbf{r})$, our calculation reconstitutes the imposed disorder potential.

Our model system comprises $N = 780$ particles confined to two dimensions and interacting *via* a inverse-twelfth power pair potential. These particles also interact with a quenched one-body disorder potential $V_d(\mathbf{r})$, modelled as a zero-mean Gaussian random field with specified variance and short-ranged spatial correlations. The interaction part of the Hamiltonian is thus: $H_{int} = \epsilon \sum_{i<j} (\frac{\sigma_0}{r_{ij}})^{12} + \sum_i V_d(\mathbf{r}_i)$. We set $\epsilon = 1$ and $\sigma_0 = 1$, thus setting energy and length scales. We use periodic boundary conditions, benchmarking our calculations in the pure limit against earlier work[15].

A one-body random Gaussian disorder potential with zero mean value and exponentially decaying correlations, $\mathrm{V}_d(\mathbf{r})$, is constructed following a method proposed by Chudnovsky and Dickman[16]. The variance (σ^2) of the Gaussian distribution and its spatial correlation length (ξ) specify the potential. We introduce disorder with a suitably small spatial correlation ($\xi = 0.12$) in units of the interparticle spacing. We study the system in the fluid regime

FIG. 2: (color-online) (a) Color plot of the configuration averaged density $\rho(\mathbf{r})$ for a single disorder configuration (see Fig 1(a)) from a portion of our simulation cell. Plot (a) shows $\rho(\mathbf{r})$ obtained from our Monte Carlo simulations using $N = 780$ particles. The averaging is over 1.41×10^5 configurations each separated by 100 MCS. The average density $\rho_0 = 0.9$. Plot (b) show the same quantity obtained from our theory for the corresponding disorder potential and ρ_0.

for $\rho_0 = 0.05, 0.3$ and 0.9, both with relatively weak ($\sigma^2 = 0.01$) and with stronger (upto $\sigma^2 = 1$) disorder. These disorder strengths are relatively moderate in comparison to the strength of the pair interaction, justifying perturbation theory in the disorder potential. We disorder average over five and ten disorder realisations for the weak and stronger disorder cases respectively, rejecting approximately the first $10^4 - 10^5$ Monte Carlo Steps (MCS). We average over about $10^3 - 10^5$ configurations each separated by 10^2 MCS, ensuring adequate thermal averaging of the local density and correlation functions.

For an equilibrium fluid in the absence of disorder, all points in space are equivalent. As a consequence, one-body distribution functions are structureless. This property does not hold, of course, *within* a particular realization of disorder. It is only restored upon a disorder average. If the fluid particles do not interact, the Boltzmann relation connects the time averaged density $\langle\rho(\mathbf{r})\rangle$ to the local potential via $\langle\rho(\mathbf{r})\rangle \sim \rho_0 \exp[-\beta V_d(\mathbf{r})]$ where ρ_0 is the average density of the fluid, $\beta = 1/k_B T$ with T the temperature, and $V_d(\mathbf{r})$ is the disorder potential. This result is valid only in the limit of vanishingly small ρ_0 or as $T \to \infty$; equivalently, in the zero correlation limit. Increasing ρ_0 *enhances* the magnitude of the signal, making it easier to observe, but at the same time introduces non-trivial correlations in particle positions. Thus, in a given disorder configuration, one-particle distributions

reflect both the inhomogeneities of the potential as well as the consequent structuring of the local density field as a consequence of correlations[14].

Figs. 2 (a) and (b) show the time averaged density $\rho(\mathbf{r})$ averaged over 1.41×10^5 independent configurations for $\rho_0 = .9$ and disorder strength $\sigma^2 = 0.1$. Note the strong structuring visible in Fig 2(a). There are pronounced, correlated peaks and troughs in the time-averaged local density, indicative both of pinning due to local potential minima as well as the indirect effects of inter-particle correlations. Figs 2(b) shows the theoretically obtained plot of $\rho(\mathbf{r})$ using a method described below. As can be seen, the theory captures the essential features of the simulation data with fair accuracy.

An inhomogeneous potential $V_d(\mathbf{r})$ couples to the local number density and can thus be absorbed into the definition of the chemical potential μ, leading to $\mu \to \mu(\mathbf{r}) = \mu + \delta\mu(\mathbf{r})$ where $\delta\mu(\mathbf{r}) = -V_d(\mathbf{r})$. The Ursell function connects the local time-averaged density $\langle\rho(\mathbf{r})\rangle$ to the inhomogeneity in the chemical potential via

$$\langle\rho(\mathbf{r})\rangle = \langle\rho_0(\mathbf{r})\rangle + \beta \int d\mathbf{r}' S(\mathbf{r},\mathbf{r}')\delta\mu(\mathbf{r}') + ..., \tag{1}$$

where $S(\mathbf{r},\mathbf{r}')$ is defined as $S(\mathbf{r},\mathbf{r}') = \langle\rho(\mathbf{r})\rho(\mathbf{r}')\rangle - \langle\rho(\mathbf{r})\rangle\langle\rho(\mathbf{r}')\rangle$[17]. Results perturbative in weak disorder are obtained by expanding about the pure limit, in which case $\langle\rho_0(\mathbf{r})\rangle = \rho_0$, the average fluid density. The density $\rho(\mathbf{r})$ can be generated if the appropriate correlations $\langle\rho(\mathbf{r})\rho(\mathbf{r}')\rangle$ and $\langle\rho(\mathbf{r})\rangle\langle\rho(\mathbf{r}')\rangle$ are available. To lowest order these are the correlations of the pure system. The results can be extended to larger disorder (a non-trivial initial $\langle\rho_0(\mathbf{r})\rangle$) provided accurate values of $S(\mathbf{r},\mathbf{r}')$ computed *in the disordered background* are available.

For weak disorder, we may approximate $\langle\rho(\mathbf{r})\rho(\mathbf{r}')\rangle - \langle\rho(\mathbf{r}\rangle\langle\rho(\mathbf{r}')\rangle$ by $\rho_0^2 h(|\mathbf{r}-\mathbf{r}'|)$ where $h(r)$ is the pair correlation function of the pure system. At somewhat stronger disorder, an alternative approach improves on this result by using the *disorder renormalized* version of these correlation functions, replacing $h(r)$ above by the function $g^{(1)}(r) - g^{(2)}(r) + \delta(\mathbf{r})/\rho_0$. Here $g^{(1)}(r)$, the disorder averaged analog of the radial distribution function, is

$$g^{(1)}(r) = [\langle\rho(0)\rho(r)\rangle]/\rho_0^2 - \delta(\mathbf{r})/\rho_0. \tag{2}$$

The analog of an Edwards-Anderson parameter reflecting the correlations of time-averaged density inhomogeneities is the "off-diagonal" distribution function $g^{(2)}(r)$, defined through

$$g^{(2)}(r) = [\langle\rho(0)\rangle\langle\rho(r)\rangle]/\rho_0^2. \tag{3}$$

Here, $\langle \dots \rangle$ denotes a thermal average for the disordered system prior to the disorder averaging, while the brackets $[\dots]$ denote an average over disorder.

Thus, in the presence of correlations, the response of the density to a nonzero external potential (apart from an overall normalization) is given by[17],

$$\langle \rho(\mathbf{r}) \rangle = \rho_0 - \beta \rho_0^2 \int d\mathbf{r}' \left(g^{(1)}(\mid \mathbf{r} - \mathbf{r}' \mid) - g^{(2)}(\mid \mathbf{r} - \mathbf{r}' \mid) \right) V_d(\mathbf{r}') - \beta \rho_0 V_d(\mathbf{r}) + \dots \quad (4)$$

At this point apart from specifying how $g^{(1)}(r)$ and $g^{(2)}(r)$ are obtained[3], which we do below, our procedure for obtaining $\rho(\mathbf{r})$ is complete. Using Eq. 4 we may obtain the density (Fig. 2 (b)) from the potential (Fig. 1(b)) or, by using a Fourier transform to invert Eq. 4, obtain the disorder potential (Fig. 1(b)) from the "experimental" density (Fig. 2(a)). In principle, inversion of the density to obtain $V_d(\mathbf{r})$ requires the specification of $g^{(2)}(r)$ which itself depends on $V_d(\mathbf{r})$. In practice, a simple iteration starting from pure system correlations converges rapidly.

Our calculation of $g^{(1)}(r)$ and $g^{(2)}(r)$ is based on an early replica-based approach to the calculation of correlation functions in a disordered fluid[3]. The replica method is applied to the partition function of a system of classical particles interacting via the Hamiltonian $H = H_{kinetic} + \frac{1}{2} \sum_{i \neq j} V(\mid \mathbf{r}_i - \mathbf{r}_j \mid) + \sum_i V_d(\mathbf{r}_i)$, with $V(r)$ is a two-body interaction potential between the particles and $V_d(\mathbf{r})$ a quenched, random, one-body potential drawn from a Gaussian distribution of zero mean and short ranged correlations: $[V_d(\mathbf{r}) V_d(\mathbf{r}')] = K(\mid \mathbf{r} - \mathbf{r}' \mid)$. One then notes that the replicated partition function resembles the partition function of a system of n "species" of particles, each labeled by an appropriate replica index, interacting via a two-body interaction which depends both on particle coordinates $(\mathbf{r}_i, \mathbf{r}_j)$ and replica indices (α, β). This system of n species of particles is considered to be a n-component mixture [17]. Taking the $n \to 0$ limit in the Ornzstein-Zernike equations governing the properties of the mixture and assuming replica symmetry, yields the following coupled set of equations, in Fourier space, coupling the pair correlation functions $h^{(1)}$ and $h^{(2)}$ to the appropriate direct correlation functions $C^{(1)}$ and $C^{(2)}$.

$$\begin{aligned} h^{(1)}(k) &= \frac{C^{(1)}(k) - [C^{(1)}(k) - C^{(2)}(k)]^2}{[1 - C^{(1)}(k) + C^{(2)}(k)]^2}, \\ h^{(2)}(k) &= \frac{C^{(2)}(k)}{[1 - C^{(1)}(k) + C^{(2)}(k)]^2}. \end{aligned} \quad (5)$$

The Fourier transforms involved are defined as $\phi(k) = \rho_0 \int d\mathbf{r} \phi(r) \exp(-i\mathbf{k} \cdot \mathbf{r})$. The replicated Ornstein-Zernike relations must be supplemented with specific closures. Previous

work applied to the problem of flux-lattice melting[18] in the presence of quenched point pinning used the simplest such closure, the Hyper-Netted Chain (HNC) closure[3]. We have experimented with a variety of closure schemes to test out the accuracy of this approach to the calculation of fluid correlations. Our best results are obtained with a closure scheme due to Rogers and Young (RY)[19] for pure systems:

$$C^{(1)}(r) = \exp\left[-\beta(V^{(1)}(r)+V^{(2)}(r))\right]\left[1+\frac{\exp\left[Y^{(1)}(r)f(r)\right]-1}{f(r)}\right]-1-Y^{(1)}(r), \quad (6)$$
$$C^{(2)}(r) = -\beta V^{(2)}(r),$$

where the function $f(r) = 1-\exp(-\alpha\, r)$ interpolates between HNC and Percus-Yevick (PY) values for large (small) r and α the "switching" parameter is chosen so as to enforce thermodynamic consistency. Here $Y^{(\nu)}(r) \equiv h^{(\nu)}(r) - C^{(\nu)}(r)$, $\nu = 1, 2$. The pair interaction potential is $V^{(1)}(r)$ and the off-diagonal potential $V^{(2)}(r)$ is the disorder averaged correlation function of the disorder potential $V_d(r)$. The integral equations for the liquid state correlations as given above must be solved numerically[3, 18, 20].

The correlation function $g^{(1)}(r)$ obtained from self-consistent solutions of the integral equations is qualitatively similar to that for the pure case at low and intermediate levels of disorder. At large values of disorder, a disorder-induced suppression of structure in $g^{(1)}(r)$ is clearly apparent. This is shown in Fig. 3(a) which exhibits the quantity $\Delta g(r) = g^{(1)}(r) - g(r)$, the difference between the pair distribution function in the disordered and pure cases. A direct comparison to the simulation data is shown in Fig. 3 (b). We find that while HNC and PY respectively under and over estimate[17] correlations, the RY closure gives very good agreement with our simulations. (This is consistent with results for the pure system.) The parameter α in the latter is taken to be its pure system value of 0.3, a value which agrees best with simulation data over the full range of densities and disorder strengths.

We show the off-diagonal correlation function $g^{(2)}(r)$ at $\sigma^2 = 0.01$ for $\rho_0 = .05, .3$ and .9 in Fig. 4(a). In the simulations, this correlation function is computed by extracting the correlations of the local time-averaged density in a particular configuration of disorder and then averaging over several disorder realizations. Correlations increase with increasing density as expected, as manifest in the oscillations of $g^{(2)}(r)$. For the same reason, the off-diagonal correlations for any density also increase with the strength of the disorder correlator (Fig. 4(b)). In both cases, our theoretical estimates based on the RY closure agree to good

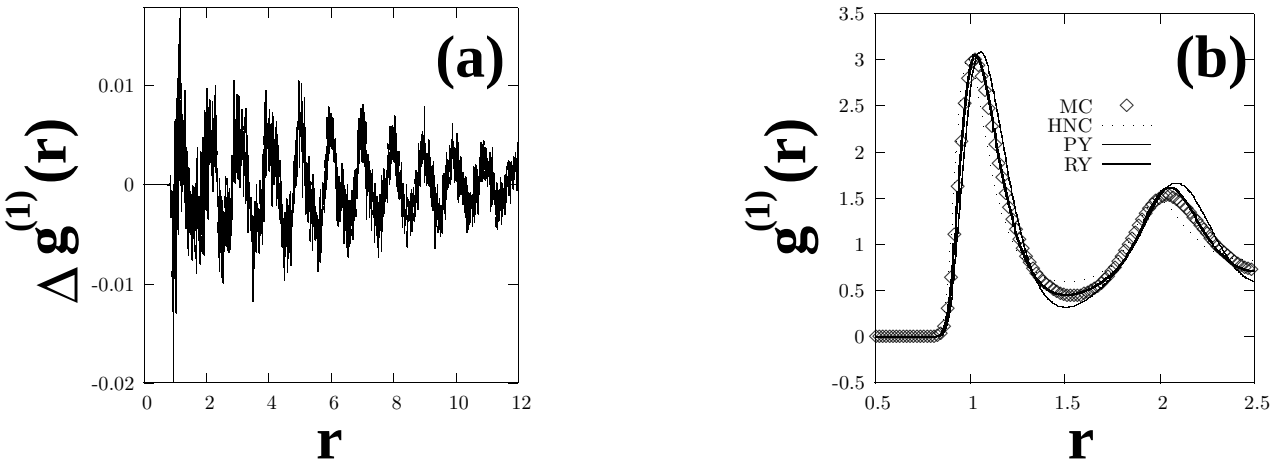

FIG. 3: (a) Plot of $\Delta g^{(1)}(r)$ for a single density $\rho_0 = 0.9$ and $\sigma^2 = 1.0$. (b) Comparison of $g^{(1)}(r)$ for density $\rho_0 = 0.9$ and $\sigma^2 = 1.0$ of simulation data (MC) with the results of HNC, PY and RY closures. Ten disorder configurations were used in the averaging.

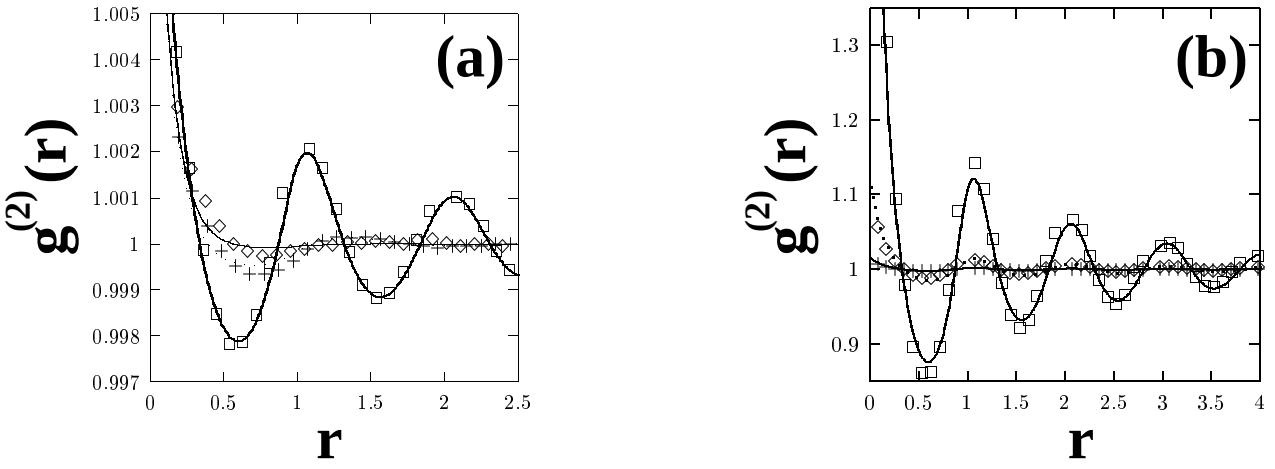

FIG. 4: (a) Plot of $g^{(2)}(r)$ comparing simulations (points) and result from the RY closure (lines) for densities $\rho_0 = .05$ (+), .3($\diamond$) and .9(box) for $\sigma^2 = .01$. Ten disorder configurations were used in the averaging. (b) Plot of $g^{(2)}(r)$ – simulations and theory (RY) for $\sigma^2 = .01$ (+), .1 ($\diamond$) and 1 (box) for $\rho_0 = 0.9$

accuracy with correlation functions obtained from the simulations.

Liquid state theory based approaches are easily adapted to a variety of different problems *vis a vis.* direct simulations. Thus, the approach presented here is potentially useful to a variety of theoretical models for experimental data. The following limitations must, however, be kept in mind: First, $\rho(\mathbf{r})$ must be accurately determined from experimental pictures for

correlations to be obtained correctly. Since the data are often thresholded, reflecting some level of coarse graining of the amplitude of the signal, a direct comparison with theory may not always be straighforward. (Interestingly, the size of the probe particles *do not* impose any theoretical limit[21] on the spatial resolution of $V_d(\mathbf{r})$ – this is limited only by the accuracy with which $\rho(\mathbf{r})$ can be imaged.) Second, our analysis neglects higher order density-density correlations. Finally, at high disorder strengths and strong correlations, the possibility exists of a transition into a state in which replica symmetry is broken, a transition which would not be captured in this calculation[22].

What types of experiments might access the unusual "off-diagonal" correlation function $g^{(2)}$? Any experiment in which repeated 'snapshots" of the system are taken, with sufficient statistics, should yield results which can be addressed by these methods. For vortices in superconductors, scanning tunneling spectroscopy[23, 24] magneto-optic imaging[11] and Lorentz and magnetic force microscopy[25, 26] can all be used as structural probes of vortex structure in thin superconducting films. Magnetic bubble domain arrays are another experimental system in which many of the features described here should be accessible [7]. We also note that several recent experiments directly access the configurations of a large number of colloidal particles confined to two dimensions [27, 28, 29, 30]. In these experiments, extensive statistics for particle positions can be generated. The colloid literature has hitherto concentrated on making substrates as homogeneous and disorder-free as possible. However, as we argue here, interacting colloidal particles moving on disordered substrates can exhibit interesting and non-trivial correlations which have not hitherto been characterized. Experimental work in this direction would be welcome.

Acknowledgements: Discussions with C. Dasgupta, S. Sastry and M. Rao and financial support from DST grant SP/S2/M-20/2001 are gratefully acknowledged.

[1] A.I. Larkin, Zh. Eksp. Teor. Fiz **58** , 1466 (1970) [Sov. Phys. JETP **31** 784 (1970)]

[2] T. Halpin-Healy and Y.-C Zhang, Phys Rep. **254**, 215 (1995)

[3] G. I. Menon and C. Dasgupta, Phys Rev. Lett, **73**, 1023, (1994)

[4] R. E. Kusner *et al*, Phys. Rev. Lett, 73, 3113(1994)

[5] R. E. Kusner, J. A. Mann, and A. J. Dahm, Phys. Rev. B **51**, 5746 (1995)

[6] K. Zahn *et al.*, Phys. Rev. Lett., **90**, 155506 (2003)

[7] R. Seshadri and R. M. Westervelt, Phys. Rev. B, **46**, 5142, (1992);*ibid.* 5150 (1992)

[8] H. Dai and C.M. Lieber, Phys. Rev. Lett, **69**, 1576, (1992)

[9] K. Harada *et. al.*, Nature, **360**, 51 (1992)

[10] A. Moser *et. al* Phys. Rev. Lett., **74**, 1847 (1995)

[11] P. E. Goa *et. al.*, Supercond. Sci. Technol., **14**, 729, (2001)

[12] A Oral *et. al.*, Supercond. Sci. Technol., **10**, 17 (1997)

[13] A. Soibel *et. al*, Nature 406, 282 (2000)

[14] C. Dasgupta and D. Feinberg, Phys. Rev. B, **57**, 11730, (1998)

[15] J. Q. Broughton, G. H. Gilmer, and J. D. Weeks, Phys. Rev. B, **25**, 4651, (1982)

[16] E. M. Chudnovsky and R. Dickman, Phys. Rev. B, **57**, 2724, (1998)

[17] J.P. Hansen and I.R. Macdonald, *Theory of Simple Liquids*, Academic, London, 2nd ed, (1986)

[18] S. Sengupta *et. al.*, Phys. Rev. Lett., **67**, 3444 (1991)

[19] F. J. Rogers and D. A. Young, Phys. Rev. A, **30**, 999 (1984)

[20] M. J. Gillan, Mol. Phys., **38**, 6, (1979)

[21] For the limiting case of $V_d(\mathbf{r}) = \delta(\mathbf{r})$, Eq. 4 gives $\rho(r \neq 0) \propto g^{(1)}(r) - g^{(2)}(r)$ which may be easily verified.

[22] F. Thalmann, C. Dasgupta and D. Feinberg, Europhys. Lett., **50**, 54 (2000)

[23] H. F. Hess *et al.*, Phys. Rev. Lett., **62**, 214 (1989)

[24] M. R. Eskildsen *et al.*, Phys. Rev. Lett, **89**, 187003, (2002)

[25] C-H Sow *et al.*, Phys. Rev. Lett., **80**, 2693, (1998)

[26] A. Volodin *et al.*, Europhys. Lett., 58, 582 (2002)

[27] C.A. Murray, W.O. Sprenger and R.A. Wenk, Phys. Rev. B **42**, 688 (1990)

[28] A.E. Larsen and D.G. Grier, Phys. Rev. Lett., **76**, 3862 (1996)

[29] K. Zahn, R. Lenke and G. Maret, Phys. Rev. Lett., **82**, 2721 (1999)

[30] P. Korda, G.C. Spalding, and D.G. Grier, Phys. Rev. B, **66**, 024504 (2002).

This figure "fig1ab.jpg" is available in "jpg" format from:

http://arXiv.org/ps/cond-mat/0410390v1

This figure "fig2ab.jpg" is available in "jpg" format from:

http://arXiv.org/ps/cond-mat/0410390v1